International Journal of Technology 12(6) 1149-1160 (2021)
Received August 2021 / Revised October 2021 / Accepted November 2021

International Journal of Technology

http://ijtech.eng.ui.ac.id

Effect of Prior Austenite Grain Size on the Annealing Twin Density and Hardness in Austenitic Stainless Steel

Mochammad Syaiful Anwar[1,2], Rana K. Melinia[1], Mayang G. Pradisti[1], Eddy S. Siradj[1*]

[1]*Department of Metallurgical and Materials Engineering, Faculty of Engineering, Universitas Indonesia, Kampus UI Depok, Depok 16424, Indonesia*
[2]*Research Center for Metallurgy and Materials, Indonesian Institute of Sciences, Kawasan PUSPIPTEK Gedung 470, Tangerang Selatan, Banten 15314, Indonesia*

Abstract. The present study examined the effect of prior austenite grain size on twin density and hardness of austenitic stainless steels (ASS). The 253 MA and 316L ASS were subjected to multi-pass cold rolling to reduce thickness up to 2.3 mm. Subsequently, the rolled steels were heat treated at 1100°C at 0, 900, 1800, 2700, and 3600 seconds in a tubular furnace in a hydrogen atmosphere. At the end of the annealing time, the rolled steel was quenched in the cooled zone of the tubular furnace until it reached room temperature in a hydrogen atmosphere. Then, microstructure observation of ASS was done to identify the austenitic grain size and annealing twin, and a hardness test was performed using the micro-Vickers hardness scale. The line intercept method was used to measure the changes in 253 MA and 316L austenitic grain sizes. ImageJ software was used to measure grain size and twin length. The results showed that austenite grains of both steels grew normally; 253 MA ASS had a lower SFE and K value than 316L ASS, which indicated that 253 MA ASS had sluggish grain growth, smaller grains, more easily formed annealing twins, and higher twin density. The Hall–Petch coefficient, K', of 253 MA ASS was higher than 316L ASS, which resulted in a higher hardness value. The Sellars, Pande and Hall-Petch models were shown to predict austenite grain sizes, twin density, and hardness in 253 MA and 316L ASS.

Keywords: 253 MA; 316L; ASS; Grain size; Micro-vickers hardness; Twin density

1. Introduction

Austenitic stainless steel (ASS) is generally employed in the construction, energy, and medical industries (Jujur et al., 2015). The thickness of this steel can be easily reduced through a deformation process at room temperature. The degree of ASS thickness reduction after cold rolling (CR) can affect the strength and ductility of the steel due to strain hardening and martensite introduced into the microstructure. However, Xu et al. (2018b) found that the increment of the grain-boundary density in the untransformed austenite structure of 316LN ASS after a high degree of CR also contributed to increased strength and decreased ductility. Subsequent annealing at a specific temperature resulted in the recrystallization of the austenite grains, which nucleated from martensite and untransformed austenite, and the grain growth process. Grain size was shown to increase with higher annealing temperature and longer duration, consequently decreasing the strength and the increasing ductility of the steel (Xu et al., 2018a).

*Corresponding author's email: siradj@metal.ui.ac.id, Tel.: +62-21-7863510
doi: 10.14716/ijtech.v12i6.5190

Studies have been performed to impede the grain growth of steels under annealing. For example, Liu et al. (2020) found that the precipitation of the M_6C pinned in the grain boundaries resulted in sluggish grain growth at a specific annealing temperature. Adabavazeh et al. (2017) found that cerium inclusions in SS400 steels resulted in decreased austenite grain growth during annealing at higher temperatures. Lee et al. (2019) discovered that ferritic stainless steels supplemented with nitrogen at around 200 ppm resulted in minimum grain sizes due to the higher pinning force of Ti-N in grain boundaries. Wu et al. (2018) found high concentrations of vanadium in the Nb-free Cr-Mo-V steels, which caused grain size to decrease. However, abnormal grain-growth behavior occurred due to V-rich M_8C_7 particles observed after the quenching process. Contrarily, Cr-Mo-V steels with the addition of niobium resulted in a precipitate of several small Nb-C particles, which significantly impacted the grain refinement. Naghizadeh and Mirzadeh (2016) reported that molybdenum content in ASS steels significantly impeded grain development during annealing at higher temperatures.

Additionally, annealing twins formed in austenite grains have been shown to depend on the migration rate of grain boundaries during recrystallization (Poddara et al., 2019). The relationship between annealing twins and grain size in austenitic stainless steels continues to interest researchers due to the presence of various alloy contents in these steels. Wang et al. (2016) clarified that the densities of grain boundaries and annealing twins increased with a small increase in grain sizes, which resulted in decreased shape of the memory effect in Fe-Mn-Si–based shape-memory alloys. Jin et al. (2015) found that the number of annealing twin boundaries of Inconel 718 did not increase with an increase in the average grain size. Bozzolo and Bernacki (2020) demonstrated several differences in twin topologies in microstructure after recrystallization and annealing. They further reported that the role of twins was not only impactful in microstructure evolution, but also affected in-service material behaviors. He et al. (2018) found that high purity Al of 25% reduction has many annealing twins grown in the early stages of recrystallization and then disappeared during grain growth. Jin et al. (2015) showed that incremental annealing twin-boundary densities in pure nickel after recrystallization were affected by prior cold deformation levels and initial grain sizes. Hajizadeh et al. (2014) indicated that that annealing twin densities appearing in brass microstructures decreased with increased grain size, as estimated using the model presented by Pande et al. (1990).

The present research studied the relationship between grain sizes, annealing twins, and the hardness of austenitic stainless steels after cold rolling and subsequent annealing with various annealing times. The aim was to clarify the effect of alloy contents in 253 MA and 316L ASS on changes in grain sizes, annealing twins, and hardness. The empirical Sellars model was used to predict grain growth. Pande et al.'s model was used to predict the annealing twin densities, and the Hall–Petch model was used to predict the hardness of the austenitic stainless steels.

2. Methods

2.1. Materials

The materials used in this study were 253 MA and 316L ASS. The chemical compositions are shown in Table 1.

Table 1 Chemical composition of ASS in this study (weight percent)

Type	C	Si	Mn	P	S	Cr	Ni	Mo	N	Ce	La	Fe
SS 253 MA	0.079	1.422	0.51	0.03	<0.005	22.06	10.86	0.08	0.384	0.03	0.014	Bal.
SS 316 L	0.012	0.3	1.67	0.035	<0.005	17.33	9.45	2.1	-	-	-	Bal.

The cold rolling process was conducted on two steel plates so that they were deformed and reach a thickness of 2.3 mm. For grain growth, each steel plate was heated in a tubular furnace at a temperature of 1100°C for 0, 900, 1800, 2700, and 3600 seconds with hydrogen (H_2) gas to prevent oxidation of the steel. After the heating, the cooling process was performed by shifting the tubular furnace from the hot zone to the cold zone until it reached room temperature. The heat treatment process is shown in Figure 1. To avoid the risk of fire or explosion during the heat treatment, H_2 gas with a pressure of less than 0.5 bar entered the quartz tube through a stainless-steel flexible hose so that the H_2 gas was not exposed to the heating coil from the furnace and flowed out of the quartz tube met the water in the glass beaker through the silicon hose. The remaining gas in the glass beaker was flowed out into the air through a nylon hose. The inlet and outlet of the quartz tube were plugged using a silicon plug connected with a stainless-steel flexible hose and a silicon hose. A manual control valve and the glass beaker's water were used to control gas from the H_2 gas cylinder. The H_2 gas cylinder was placed outside the laboratory, which was separated by a brick wall. The specimens were entered and taken out from the quartz tube at room temperature.

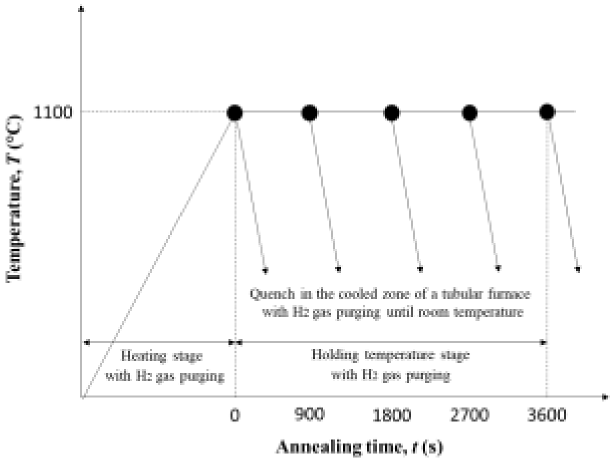

Figure 1 Experimental heat treatment process

After the heat treatment process, the quenched samples were polished by conventional techniques and etched in a solution containing 4-parts HCl plus 1-part HNO_3 on volume basis for about 18–60 s to reveal the austenite grain boundaries. Then, hardness testing was conducted using a micro-Vickers machine with a load of 0.3 N. The actual austenite grain sizes were determined according to ASTM E112 using the line intercept method. ImageJ software was used to measure grain size and twin length with Magnificent 100×.

2.2. Size of Dataset

The stacking-fault energy (SFE) value was determined using Schramm and Reed's equation, which is shown below (Equation 1; Schramm and Reed, 1975):

$$SFE = -53 + 6.2(\%Ni) + 0.7(\%Cr) + 3.2(\%Mn) + 9.3(\%Mo) \tag{1}$$

The grain growth of austenitic steel 253 MA and 316L can be predicted by employing the Sellars model. The average grain size can be calculated using Equation 2:

$$d^n - d_0{}^n = K \cdot t \tag{2}$$

where d is the average grain diameter, d_0 represents the initial grain diameter, n is a constant exponent for grain-growth kinetics, t is annealing time, and K is a constant.
The constant K can be calculated using Equation 3:

$$K = k_0\, EXP\left(-\frac{Q}{RT}\right) \tag{3}$$

where k_0 is a constant, T represents the specific heating temperature in Kelvin, R is the universal gas constant, 8.31 J/(mol•K), and Q is the activation energy for grain growth (J/mol) (Xu et al., 2017).

The prediction of the relationship between annealing twin density and the grain size of stainless steels 253 MA and 316L can be calculated utilizing the Pande et al.'s model. Annealing twin density can be calculated using Equation 4:

$$\frac{P}{P_0} = \frac{D_0}{D} log\left(\frac{D}{D_0}\right) \tag{4}$$

where p_0 and D_0 represents constants independent of temperature, D is the grain size, and p is the twin density (Pande et al., 1990).

The Hall-Petch model in the Equation 5 was used to calculate the relationship between hardness value and grain growth.

$$H = H_0 + k' \cdot d^{-1/2} \tag{5}$$

where H_0 is the intrinsic hardness of ASS, k' represents the Hall-Petch coefficient, and d is the average grain diameter (Huang et al., 2019).

Regression was used to obtain the coefficient value using the Solve–Excel software.

3. Results and Discussion

3.1. Grain Growth of 253 MA and 316L ASS

The average grain sizes of 253 MA and 316L ASS after cold rolling and annealing at 1100°C for 0 to 3600 seconds are shown in Table 2 and Figure 2.

Table 2 Average grain size of 253 MA dan 316L ASS (in µm)

Annealing time (s)	SS 253 MA	Standard deviation	SS 316L	Standard deviation
0	13.54	0.87	14.93	1.7
900	17.07	0.5	23.56	2.05
1800	19.76	1.6	26.19	1.95
2700	20.91	1.4	28.98	3.27
3600	24.5	1.01	29.28	2.59

The grain sizes of two steel plates increased gradually with annealing time; however, 253 MA ASS had a lower grain size than 316L ASS under annealing. The high contents of Cr, Ni, and N in 253 MA ASS caused increased strength through cold rolling to ensure that reducing the thickness of 253 MA ASS would be more difficult to accomplish than reducing the thickness of 316L ASS. The present work is related to a previous study by Ilola et al. (1998). The high alloy contents might also result in a high degree of strain-induced martensite (SIM) and undeformed austenite in 253 MA ASS microstructures after cold rolling. Next, the SIM was transformed to austenite very slowly under recrystallization, which resulted in sluggish grain growth. However, nitrogen in 253 MA ASS can promote the grain growth of austenite (Staśko et al., 2006), cerium and lanthanum, as micro-alloying can be precipitated in grain boundaries resulting in inhibited grain growth (Dani et al., 2018; Zhou et al., 2020). Previous works have also shown that V, Nb, and Ti have micro-alloyed retarded austenite grain growth (Staśko et al., 2006; Karmakar et al., 2014). Additionally, 316L ASS in this work has a high content of molybdenum, but it was not sufficient to suppress grain growth compared to 253 MA ASS during annealing. Han et al. (2015) found that molybdenum at around 2 wt% in IN718 alloy could precipitate in austenite grain boundaries, which effectively prevented grain growth.

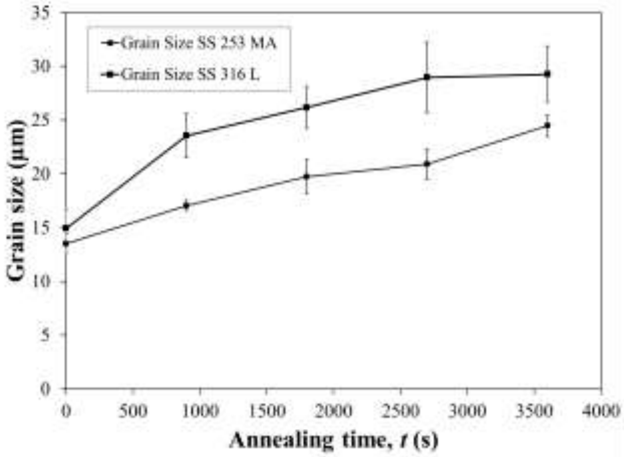

Figure 2 Comparison of grain size of SS 253 MA and SS 316L after cold rolling and annealing at 1100°C

Grain growth is also affected by the SFE values in both steels. SFE is a value that expresses the dissolved particles or partially dispersed dissolved particles in the solid solution of a steel microstructure after the annealing process (Padilha et al., 2003). The high and low values of SFE can affect dislocation mobilities, SIM, grain size, and twinning. The SFE calculation results are presented in Table 3, which shows that the SFE value of 253 MA ASS was lower than 316L ASS, indicating that more refined austenite grain sizes developed in the microstructures.

Table 3 SFE values of 253 MA and 316 L stainless steel

Type	UNS	SFE
SS 253 MA	S30815	32.1
SS 316L	S31603	42.6

The grain growth of 253 MA and 316L ASS can be predicted with the Sellars model, and the average grain size can be calculated using Equation 2. The values of constants such as *n*, *K*, and *Q* in the Sellars model depend on the type of metal undergoing the grain growth process. Table 4 shows the constants *n* and *K* of the 253 MA and 316L ASS. In the present study, the *n* value of 2.52 and 2.48 were close to the values reported in previous studies (Kim et al., 2013). This implies that the austenite grains of both steels grew normally. The *K* values represented grain growth kinetics of the steels (Moravec et al., 2019). The *K* value of 253 MA being lower than the value of 316L ASS indicated that austenite grains in 253 MA ASS grew more slowly than in 316L ASS with annealing time.

Table 4 Calculation results for constants *n* and *K*

Type	n	K
SS 253 MA	2.52	0.62
SS 316L	2.48	1.2

The actual and predicted grain size of 253 MA and SS 316L ASS are shown in Figure 3. In this figure, the predicted grain sizes are close to the actual grain sizes, which means that the Sellars model predicted austenite grain growth of 253 MA and 316L ASS during annealing.

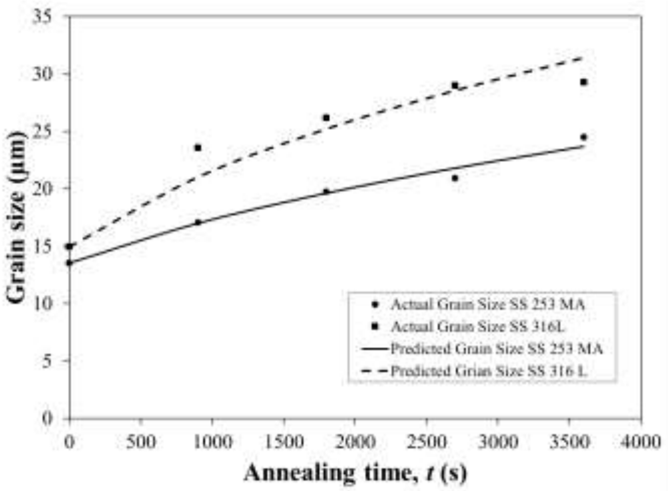

Figure 3 Comparison of the average grain sizes of SS 253 MA and SS 316L between the actual values and estimated values of Sellars model

3.2. Effect Grain Size on the Annealing Twin

Figure 4 shows the annealing twins of both steels after annealing at 1100°C for 1800 s. As a theory, annealing twin length increases with increased grain sizes, while annealing densities increase inversely with grain sizes under annealing. According to Meyers and McCowan, three models can explain the occurrence of annealing twins: growth accident models, grain encounter models, and models involving the nucleation of twins by stacking faults or fault packets. The growth accident model is commonly used to explain the formation of annealing twins occurring in grain-boundary migration caused by stacking errors during grain growth (Meyers and McCowan, 1986; Jin et al., 2016).

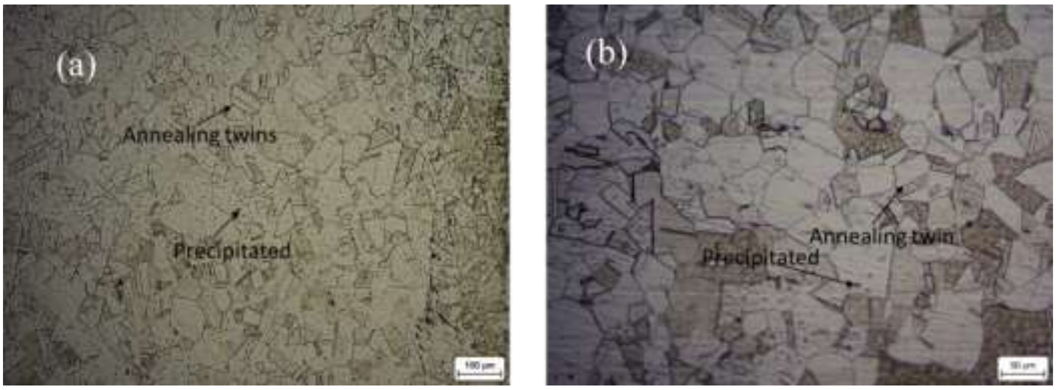

Figure 4 Annealing twins in 253 MA and 316L ASS after annealing at 1100°C for 1800 s

However, Figure 4 shows that some of the annealing twin lengths did not fully extend across the austenite grains of both steels. These results indicated that the annealing twins attached to the austenite grains could change by the migration of the grain boundaries during the grain-growth process (Wang et al., 2020). Figure 5 shows the relationship between the twin lengths and grain sizes of both steels. In this figure, the twin lengths of the austenite grain of 253 MA ASS increase gradually until the grain sizes are around 20 µm, after which a slight decrease in their lengths can be noted, particularly when the grain becomes coarser. These results were likely due to the decreased frequency of annealing twins during grain growth (Chen et al., 2015). Additionally, twin lengths in the austenite grain of 316L ASS slightly decreased the grain sizes to 26 µm, after which, inconsistent twin lengths occurred in the coarser grains. This was likely because of low grain-boundary energy in 316L ASS during recrystallization, resulting in few nucleations of twins (Varin and Kruszynska, 1987).

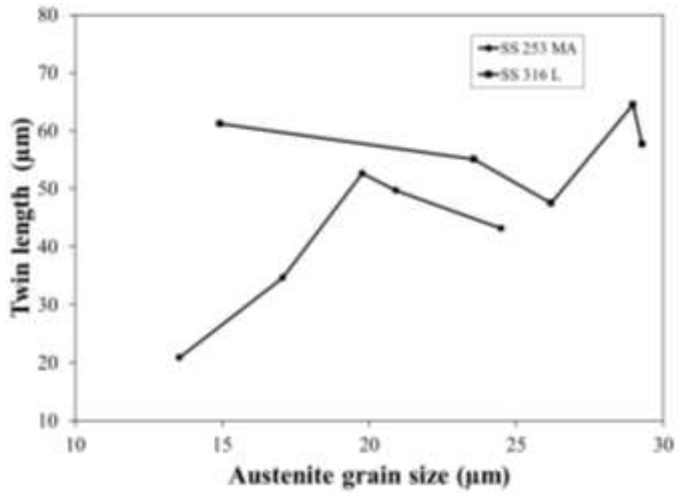

Figure 5 Relationship between twin length and grain size of 253 MA and 316L ASS

The relationship between the annealing twin densities and grain sizes of both steels can be calculated using Equation 4. Table 5 shows the constant values of p_0 and D_0 of both steels.

Table 5 The results of the calculation of the constants p_0 and D_0

Type	p_0	D_0
SS 253 MA	585	0.003
SS 316L	1.84	1.13

The actual and the predicted annealing twin densities of 253 MA ASS and 316L ASS are shown in Figure 6.

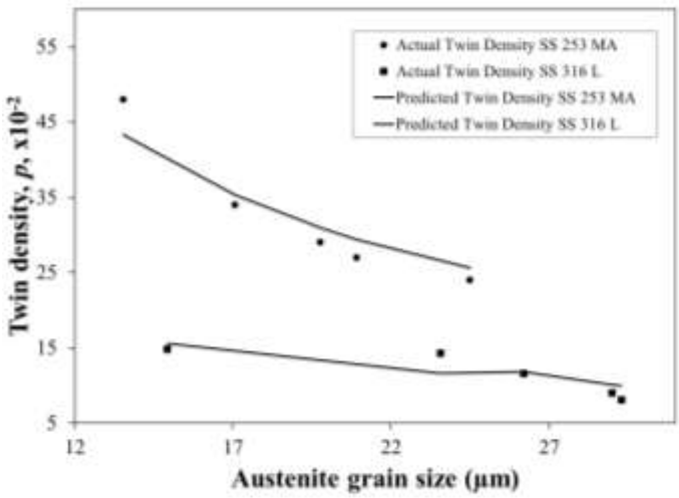

Figure 6 Comparison of twin densities of 253 MA and 316L ASS between the actual values and predicted values of the model by Pande et al. (1990)

In this figure, the annealing twin densities decrease with increased grain sizes, while the frequency of the annealing twin densities in 253 MA ASS is higher than in 316L ASS. These results indicate that a low SFE in 253 MA ASS (Table 3) results in easily formed annealing twins during annealing after deformation and internal stress release, as reflected in a twin formed under annealing (Song et al., 2019). The predicted annealing twin densities were close to the actual annealing twin densities. This implies that the model by Pande et al. (1990) can predict the annealing twin density of 253 MA and 316L ASS during grain growth.

3.3. *Effect of Grain Size on Hardness*

Figure 7 shows the micro-Vickers hardness value of 253 MA and 316L ASS after annealing several times. In this figure, the micro-Vickers hardness value of both steels decreases slightly with increased annealing time. In the previous work by Tucho and Hansen (2021), the hardness also decreased with increased holding time, but increased the same hardness value in the specific long-hold time. The decreased hardness reflects a change in microstructure as it becomes coarse and the ductility increases (Xu et al., 2018a). Additionally, the precipitation of metal carbide or nitride might occur in the grains of both steels and insignificantly contribute to the decreased hardness value. The difference in hardness is presumably due to differences in recrystallization evolutions (Ashtiani and Karami, 2015). The degree of recrystallization and after-grain growth may be affected by the amount of strain-induced martensite, precipitation, micro-alloying, and percentage of Cr, Ni, Mo, and N contents (Naghizadeh and Mirzadeh, 2016; Adabavazeh et al., 2017; Wu et al., 2018; Lee et al., 2019; Liu et al., 2020). Recrystallization, which develops fine grains in the steel, results in a higher hardness value. According to a previous study, hardness increases with increased indentation depth at a specific range in the small grain size due to the grain boundary (GB) effect. Such grain boundaries (GBs) have been regarded as obstacles to dislocation motion or as a source of dislocations. The dislocation is generated in regions close to the GBs. Hence, higher stress is required to move dislocations (Hall, 1951; Jung et al., 2013). As shown in Figure 8, the finer grain of austenite considered with high $d^{-0.5}$ value resulted in increased hardness values in both steels. When the grain size increased, the number of grain boundary areas decreased so that the hardness decreased.

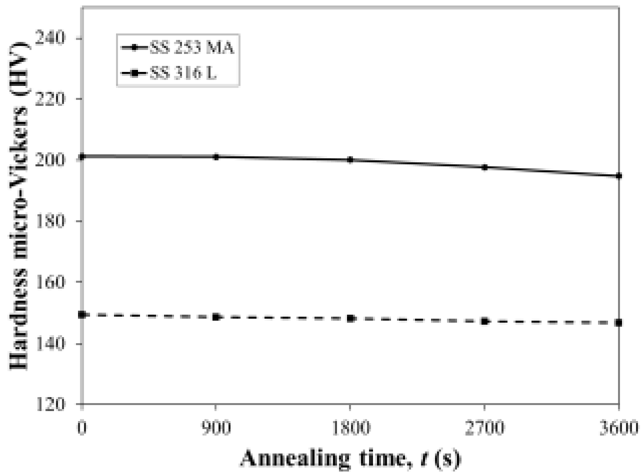

Figure 7 Comparison of micro-Vicker hardness value vs. annealing time between 253 MA and 316L ASS

The Hall–Petch model was used to calculate the relationship between hardness value and grain size. The coefficients of H_0 and k' were calculated according to Equation 5. The previous literature reported that the k' value was correlated with the shear modulus of alloys, which describes dislocation behavior in the microstructure of alloys (Huang et al., 2019). Table 6 shows the constant values of H_0 (178.5) and k' (88.5) in 253 MA steel were higher than 316L steel. This indicated that 253 MA ASS had a higher shear modulus, resulting in a higher hardness value.

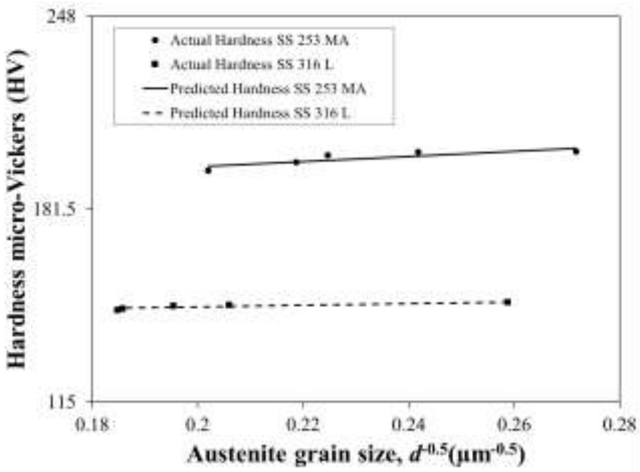

Figure 8 Comparison of hardness micro-Vickers of 253 MA and 316L ASS between the actual values and predicted values using Hall-Petch model

The experimental hardness value and the predicted hardness value are shown in Figure 8. Based on this figure, the predicted value is almost close to the experimental value. This indicated that the Hall–Petch model was able to predict the hardness values of 253 MA and 316L ASS.

Table 6 The results of the calculation of the constants H_0 and k'

Type	H_0	k'
SS 253 MA	178.5	88.5
SS 316L	141.8	30.05

4. Conclusions

To study the effect of prior austenite grain size on the annealing twin density and hardness, cold-rolled 253 MA and 316L ASS were heated at 1100°C for various annealing durations. Experimental results indicated that grain size increased with increased annealing time. Normal growth occurred in the austenite grain of both steels. The low SFE and K values in 253 MA ASS resulted in sluggish grain growth, smaller grains, easier formation of annealing twins, and higher twin density than in 316L ASS. Higher Hall–Petch coefficients, k', in 253 MA ASS caused higher shear modulus as well as hardness value than in 316L ASS. Therefore, the Sellars, Pande, and Hall–Petch models were shown to predict grain growth, twin density, and hardness in both 253 MA and 316L ASS.

Acknowledgements

The authors would like to express their gratitude to the Ministry of Research and Technology/National Research and Innovation Agency Indonesia and the Indonesian Institute of Sciences (LIPI) for financial support for PUTI Doktor 2020 with contract number NKB-3355/UN2.RST/HKP.05.00/2020, as well as LIPI Research with contract number SK 197/H/2019. We would also like to thank PT. Cahaya Bina Baja-Sandvik, who supported the procurement of the stainless steel 253 MA.

References

Adabavazeh, Z., Hwang, W.S., Dezfoli, A.R.A., 2017. Pinning Effect of Cerium Inclusions during Austenite Grains Growth in SS400 Steel at 1300°C: A Combined Phase Field and Experimental Study. *Crystals*, Volume 7(10), pp. 1–9

Ashtiani, H.R.R., Karami, P., 2015. Prediction of the Microstructural Variations of Cold-Worked Pure Aluminum during Annealing Process. *Modeling and Numerical Simulation of Material Science*, Volume 5, pp. 1–14

Bozzolo, N., Bernacki, M., 2020., Viewpoint on the Formation and Evolution of Annealing Twins During Thermomechanical Processing of FCC Metals and Alloy. *Metallalurgical and Materials Transaction A*, Volume 51, pp. 2665–2684

Chen, X.P., Li, L.F., Sun, H.F., Wang, L.X., Liu, Q., 2015. Studies on the Evolution of Annealing Twins during Recrystallization and Grain Growth in Highly Rolled Pure Nickel. *Materials Science and Engineering: A*, Volume 622, pp. 108–113

Dani, M., Parikin, Dimyati, A., Rivai, A.K., Iskandar, R., 2018. A New Precipitation-Hardened Austenitic Stainless Steel Investigated by Electron Microscopy. *International Journal of Technology*, Volume 9(1), pp. 89–98

Hajizadeh, K., Tajjaly, M., Emadoddin, E., Borhani, E., 2014. Study of Texture, Anisotropy and Formability of Cartridge Brass Sheets. *Journal of Alloys and Compounds*, Volume 588, pp. 690–696

Hall, E.O., 1951. The Deformation and Aging of Mild Steel: III Discussion of Results. *In:* Proceeding of Physical Society Section B, Volume 64(9), p. 747

Han, D.W., Liu, F., Jia, D., Qi, F., Yang, H.C., Sun, W.R., Hu, Z.Q., 2015. Effect of Mo Addition on the Grain Growth of IN718 Alloy. *Materials Science Forum*, Volume 816, pp. 594–600

He, Q., Huang, T., Shuai, L., Zhang, Y., Wu, G., Huang, X., Jensen, D.J., 2018. In-Situ Investigation of the Evolution of Annealing Twins in High Purity Aluminium. *Scripta Materialia*, Volume 153, pp. 68–72

Huang, Y.-C., Su, C.-H., Wu, S.-K., Lin, C., 2019. A Study on the Hall–Petch Relationship and Grain Growth Kinetics in FCC-Structured High/Medium Entropy Alloys. *Entropy*, Volume 21(3), pp. 1–13

Ilola, R., Hänninen, H., Kauppi, T., 1998. Hot and Cold Rolling of High Nitrogen Cr-Ni and Cr-Mn Austenitic Stainless Steels. *Journal of Materials Engineering and Performance*, Volume 7(5), pp. 661–666

Jin, Y., Bernacki, M., Agnoli, A., Lin, B., Rohrer, G., Rollett, A., Bozzolo, N., 2016. Evolution of the Annealing Twin Density during δ-Supersolvus Grain Growth in the Nickel-Based Superalloy Inconel™ 718. *Metals*, Volume 6(1), pp. 1–13

Jin, Y., Lin, B., Rollette, A.D., Rohrer, G.S., Bernacki, M., Bozzolo, N., 2015. Thermo-Mechanical Factors Influencing Annealing Twin Development in Nickel During Recrystallization. Journal of Materials Science, Volume 50(15), pp. 5191–5203

Jujur, I.N., Joni, S., Bakri, A., Wargadipura, A.H.S., 2015. Analysis of Oxide Inclusions on Medical Grade 316L Stainless Steel using Local Raw. *International Journal of Technology*, Volume 6(7), pp. 1184–1190

Jung, B., Lee, H., Park, H., 2013. Effect of Grain Size on the Indentation Hardness for Polycrystalline Materials by the Modified Strain Gradient Theory. *International Journal of Solids and Structures*, Volume 50(18), pp. 2719–2724

Karmakar, A., Kundu, S., Roy, S., Neogy, S., Srivastava, D., Chakrabarti, D., 2014. Effect of Microalloying Elements on Austenite Grain Growth in Nb–Ti and Nb–V Steels. *Materials Science and Technology*, Volume 30(6), pp. 653–664

Kim, B.N., Hiraga, K., Morita, K., 2003. Kinetics of Normal Grain Growth Depending on the Size Distribution of Small Grains. *Materials Transactions*, Volume 44(11), pp. 2239–2244

Lee, M.H., Kim, R., Park, J.H., 2019. Effect of Nitrogen on Grain Growth and Formability of Ti-Stabilized Ferritic Stainless Steels. *Scientific Reports*, Volume 9(6369), pp. 1–11

Liu, Z., Tu, X., Wang, X., Liang, J., Yang, Z., Sun, Y., Wang, C., 2020. Carbide Dissolution and Austenite Grain Growth Behavior of a New Ultrahigh-Strength Stainless Steel. *Journal of Iron and Steel Research International*, Volume 27, pp. 732–741

Meyers, M.A., McCowan, C., 1986. Interface Migration and Control of Microstructure. *In:* Proceedings of an International Symposium Held in Conjunction with ASM's Metals Congress and TMS/AIME Fall Meeting, Detroit, Michigan, USA, pp. 17–21

Moravec, J., Novakova, I., Sobotka, J., Neumann, H., 2019. Determination of Grain Growth Kinetics and Assessment of Welding Effect on Properties of S700MC Steel in the HAZ of Welded Joints. *Metals*, Volume 9(6), pp. 1–20

Naghizadeh, M., Mirzadeh, H., 2016. Elucidating the Effect of Alloying Elements on the Behavior of Austenitic Stainless Steels at Elevated Temperatures. *Metallalurgical and Materials Transaction A*, Volume 47(12), pp. 5698–5703

Padilha, A.F., Plaut, R.L., Rios, P.R., 2003. Annealing of Cold-worked Austenitic Stainless Steels. *ISIJ International*, Volume 43(2), pp. 135–143

Pande, C.S., Imam, M.A., Rath, B.B., 1990. Study of Annealing Twins in FCC Metals and Alloys. *Metallurgical Transactions A*, Volume 21A, pp. 2891–2896

Poddara D., Chakrabortya A., Kumar R.B., 2019. Annealing Twin Evolution in the Grain Growth Stagnant Austenitic Stainless Steel Microstructure. *Materials Characterization*, Volume 155, https://doi.org/10.1016/j.matchar.2019.109791

Song, G., Kaisheng, J., Song, H., Zhang, S., 2019. Microstructure Transformation and Twinning Mechanism of 304 Stainless Steel Tube During Hydraulic Bulging. *Materials Research Express*, Volume 6(12), pp. 1–12

Staśko, R., Adrian, H., Adrian, A., 2006. Effect of Nitrogen and Vanadium on Austenite Grain Growth Kinetics of a Low Alloy Steel. *Materials Characterization*, Volume 56(4), pp. 340–347

Tucho, W.M., Hansen, V., 2021. Studies of Post-Fabrication Heat Treatment of L-PBF-Inconel 718: Effects of Hold Time on Microstructure, Annealing Twins, and Hardness. *Metals*, Volume 11(2), pp. 1–19

Varin, R.A., Kruszynska, J., 1987. Control of Annealing Twins in Type 316 Austenitic Stainless Steel. *Acta Metallurgica*, Volume 35(7), pp. 1767–1774

Wang, G., Peng, H., Zhang, C., Wang, S., Wen, Y., 2016. Relationship Among Grain Size, Annealing Twins and Shape Memory Effect in Fe–Mn–Si Based Shape Memory Alloys. *Smart Materials and Structures*, Volume 25(7), pp. 1–9

Wang, S.W., Song, H.W., Chen, Y., Zhang, S.H., Li, H.H., 2020. Evolution of Annealing Twins and Recrystallization Texture in Thin-Walled Copper Tube During Heat Treatment. *Acta Metallurgica Sinica (English Letters),* Volume 33, pp. 1618–1626

Wu, D., Wang, F., Cheng, J., Li, C., 2018. Effect of Nb and V on Austenite Grain Growth Behaviour of the Cr-Mo-V Steel for Brake Discs. High Temperature *Material and Process*, Volume 37(9–10), pp. 899–907

Xu, D., Ji, C., Zhao, H., Ju, D., Zhu, M., 2017. A New Study on the Growth Behavior of Austenite Grains During Heating Processes. *Scientific Reports*, Volume 7(1), 3968

Xu, D., Wan, X., Yu, J., Xu, G., Li, G., 2018a. Effect of Cold Deformation on Microstructures and Mechanical Properties of Austenitic Stainless Steel. *Metals*, Volume 8(7), pp. 1–14

Xu, D.M., Li, G.Q., Wan, X.L., Misra, R.D.K., Zhang, X.G., Xu, G., Wu, K.M., 2018b. The Effect of Annealing on the Microstructural Evolution and Mechanical Properties in Phase Reversed 316LN Austenitic Stainless Steel. *Materials Science and Engineering: A*, Volume 720(10), pp. 36–48

Zhou, W., Zhu, J., Zhang, Z., 2020. Austenite Grain Growth Behaviors of La-Microalloyed H13 Steel and Its Effect on Mechanical Properties. *Metallurgical and Materials Transactions A*, Volume 51, pp. 4662–4673